Title: Short-term social isolation acts on hypothalamic neurons to promote social behavior in a sex- and context-dependent manner.

Xin Zhao[1], Yurim Chae[1], Destiny Smith[1], Valerie Chen[1], Dylan DeFelipe[1], Joshua W Sokol[1], Archana Sadangi[1], and Katherine Tschida[1]

[1]Department of Psychology, Cornell University, Ithaca NY 14853

*Corresponding Author: Katherine Tschida, kat227@cornell.edu

Abstract

Social animals, including both humans and mice, are highly motivated to engage in social interactions. Short-term social isolation increases social motivation and promotes social behavior, but the neural circuits through which it does so remain incompletely understood. Here, we sought to identify neurons that promote social behavior in single-housed female mice, which exhibit increased rates of social investigation, social ultrasonic vocalizations (USVs), and mounting during same-sex interactions that follow a period of short-term (3-day) isolation. We first used immunostaining for the immediate early gene Fos to identify a population of neurons in the preoptic hypothalamus (POA) that increase their activity in single-housed females following same-sex interactions (POA_{iso} neurons). TRAP2-mediated chemogenetic silencing of POA_{iso} neurons in single-housed females significantly attenuates the effects of short-term isolation on social investigation and USV production and also tends to reduce mounting. In contrast, caspase-mediated ablation of POA_{iso} neurons in single-housed females robustly attenuates mounting but has no effect on social investigation or USV production. Optogenetic activation of POA_{iso} neurons in group-housed females promotes USV production but does not recapitulate the effects of short-term isolation on social investigation and mounting. To understand whether a similar population of POA_{iso} neurons promotes social behavior in single-housed males, we performed Fos immunostaining in single-housed males following either same-sex or opposite-sex social interactions. These experiments revealed a population of POA neurons that increase Fos expression in single-housed males following opposite-sex, but not same-sex, interactions. Chemogenetic silencing of POA_{iso} neurons in single-housed males during interactions with females tends to reduce mounting but does not decrease social investigation or USV production. These experiments identify a population of hypothalamic neurons that promote social behavior following short-term isolation in a sex- and social context-dependent manner.

Keywords: social isolation, ultrasonic vocalization, preoptic hypothalamus, mounting, female

Introduction

Humans and other social mammals find social interactions rewarding and are highly motivated to seek out social connections. Consequently, the experience of social isolation is aversive and impacts both our brains and our behaviors. While long-term isolation can lead to the emergence of anti-social behaviors in both humans and rodents (An et al., 2017; Arrigo and Bullock, 2008; Check et al., 1985; Hossain et al., 2020; Killgore et al., 2021; Ma et al., 2011, 2022; Machimbarrena et al., 2019; Matsumoto et al., 2005; Mears and Bales, 2009; Reid et al., 2022; Toth et al., 2011; Valzelli, 1973; Weiss et al., 2004; Wiberg and Grice, 1963; Zelikowsky et al., 2018), short-term isolation typically increases levels of social motivation and promotes social-seeking behaviors (Baumeister and Leary, 1995; Cacioppo et al., 2006; Cacioppo and Cacioppo, 2018; House et al., 1988; Lee et al., 2021; Niesink and van Ree, 1982; Panksepp and Beatty, 1980; Zhao et al., 2021). Alterations in social motivation are characteristic of many neurodevelopmental disorders, including autism spectrum disorder (Chevallier et al., 2012; Clements et al., 2018). How short-term social isolation acts on the brain to promote social behavior remains incompletely understood.

Mesolimbic circuits play an important role in regulating social motivation and social reward, during courtship as well as during same-sex interactions (Bariselli et al., 2018; Dai et al., 2022; Dölen et al., 2013; Gunaydin et al., 2014; Hung et al., 2017; Love, 2014; Melis et al., 2022; Resendez et al., 2020; Robinson et al., 2011; Solié et al., 2022; Tang et al., 2014; Walum and Young, 2018; Xiao et al., 2017). In line with their role in regulating social behavior, changes in the function of mesolimbic circuits have been reported following long-term (weeks-long) social isolation and/or early-life social isolation (McWain et al., 2022; Musardo et al., 2022; Tan et al., 2021; Yorgason et al., 2016). The neural circuit changes that mediate the effects of short-term isolation on social motivation in adult animals are comparatively less explored, but here as well, recent studies in both humans and rodents have implicated changes in various populations of midbrain dopamine neurons (Inagaki et al., 2016; Matthews et al., 2016; Tomova et al., 2020). Beyond its effects on mesolimbic circuits, whether social isolation acts on additional neuronal populations to promote social interaction is unknown.

In recent work, we found that short-term (3-day) social isolation exerts robust effects on the social behaviors of C57BL/6J female mice (Zhao et al., 2021). Relative to group-housed females, single-housed females that subsequently engaged in same-sex interactions exhibited increased rates of social investigation, increased rates of USVs, and were also observed to mount female social partners, a behavior never observed in pairs of group-

housed females (Zhao et al., 2021). The robust effect of short-term isolation on these three aspects of female social behavior provides a powerful paradigm to identify neurobiological changes that mediate the effects of short-term isolation on social behavior. In the current study, we combined this behavioral paradigm with Fos immunostaining and the TRAP2 activity-dependent labeling approach (Allen et al., 2017; DeNardo et al., 2019) to identify and characterize a population of neurons in the preoptic hypothalamus that increase their activity in single-housed females following same-sex social interactions (i.e., POA_{iso} neurons). We next asked whether silencing or ablation of POA_{iso} neurons attenuates the effects of short-term isolation on female social behavior, and whether artificial activation of POA_{iso} neurons in group-housed females mimics the effects of short-term isolation on female social behavior. Finally, we extended a subset of these experiments to single-housed males engaged in opposite-sex and same-sex interactions, to understand whether short-term isolation acts on the POA to promote social behavior in a manner that depends on either sex or social context. This study identifies novel neurobiological mechanisms through which short-term social isolation acts on the brain to promote social interaction. Our findings also add to an emerging literature indicating that the POA regulates not only sexual behavior but also female social behavior during same-sex interactions.

Results

Neurons in the preoptic hypothalamus increase their activity in socially isolated female mice following same-sex social interactions

To identify changes in neuronal activity that may underlie the effects of short-term isolation on female social behavior, we performed immunostaining for the immediate early gene Fos in brain sections collected from group-housed and single-housed (3-days) subject females following 30-minute social encounters in their home cages with a novel, group-housed visitor female (Fig. 1A). In line with our previous behavioral findings (Zhao et al., 2021), we observed that single-housed female residents spent more time investigating visitors (Fig. 1B; Mann-Whitney U test, $p = 0.001$) and in many trials mounted visitors, a behavior that was not observed in group-housed residents (Fig. 1C; 0 of 12 group-housed residents and 10 of 13 single-housed residents mounted visitors; Mann-Whitney U test for difference in total mounting duration, $p < 0.001$; see Table S1 for complete statistical details). Female pairs that contained a single-housed resident also produced higher rates of ultrasonic vocalizations (USVs) than pairs with a group-housed resident (Fig. 1D; Mann-Whitney U test, $p < 0.001$). Although either female in a dyad can produce USVs (Warren et al., 2020), the robust effects of short-term isolation on the non-vocal social behaviors of single-housed females suggest that at least some of the elevation in USV rates is driven by

increased USV production by the single-housed resident. Given the robust effects of short-term isolation on these three aspects of female social behavior, we focused our analyses on two hypothalamic regions implicated in regulating these behaviors: the preoptic area (POA), which regulates social approach (McHenry et al., 2017), social reward (Hu et al., 2021), mounting (Floody, 1989; Karigo et al., 2021; Wei et al., 2018) and USV production (Chen et al., 2021; Gao et al., 2019; Green et al., 2018; Karigo et al., 2021; Michael et al., 2020); and the ventromedial hypothalamus (VMH), which regulates mounting (Hashikawa et al., 2017; Karigo et al., 2021; Lee et al., 2014; Liu et al., 2022). We also examined Fos expression within the caudolateral periaqueductal gray (PAG), based on the well-established role of this region in the control of vocalization in vertebrates and USV production in mice (Chen et al., 2021; Jürgens, 1994; Michael et al., 2020; Tschida et al., 2019). To test whether any observed differences in Fos expression in these three regions were associated with isolation-induced changes in social behavior rather than baseline differences between groups, we also measured Fos expression in the POA, the VMH, and the PAG of group-housed and single-housed females that did not engage in social interaction with novel female visitors (Fig. 1E-F; Fig. S1).

These analyses revealed that baseline levels of Fos expression within the POA and the VMH did not differ between group-housed and single-housed females (Fig. 1F, left and middle, open bars; two-way ANOVA to analyze Fos expression within each brain region, factor 1 = housing status, factor 2 = social interaction, followed by post-hoc Tukey's HSD tests). Following social interactions with novel female visitors, single-housed females exhibited robust increases in Fos expression within the POA (Fig. 1F, left; $p < 0.001$) but not within the VMH (Fig. 1F, middle; $p > 0.05$). In contrast, Fos expression within these two brain areas did not increase significantly in group-housed females that interacted with novel female visitors (Fig. 1F; $p > 0.05$ for both comparisons). Similar to the POA, baseline Fos expression within the PAG did not differ between group-housed and single-housed females ($p > 0.05$), and only single-housed females displayed increased PAG Fos expression following social interactions with novel female visitors (Fig. 1F, right; $p < 0.001$), a finding that further supports the idea that single-housed females increase USV production during same-sex interactions. POA Fos expression was significantly and positively correlated with the total amount of time spent in resident-initiated investigation for both group-housed and single-housed females (Fig. S1C, left; linear regression, $p < 0.05$), as well as with the total number of mounting bouts produced by single-housed resident females (Fig. S1C, middle; $p < 0.01$). In both group-housed and single-housed female residents, Fos expression tended to correlate positively with total USVs, but these relationships were not significant (Fig. S1C, right; $p > 0.05$ for both comparisons; see Fig. S1D-E for relationships of VMH Fos and PAG Fos to vocal and non-vocal social behaviors). In summary, POA Fos expression increases

selectively in single-housed females following social interactions, and levels of POA Fos expression are also well related to the production of specific types of social behaviors by single-housed females.

To ask whether the effects of short-term isolation on female social behavior and POA Fos expression are long-lasting, we measured social behaviors of female residents at three timepoints: (1) on day 0, when female subjects were still group-housed; (2) on day 3, after female subjects had been single-housed for 3 days; and (3) on day 17, after half of the subject females had been re-group-housed with their same-sex siblings for two weeks and the other half of the subject females remained single-housed for two weeks (Figs. 1G-I). Brains of re-group-housed and 14-day single-housed subject females were collected after the day 17 social interaction, and Fos expression within the POA was examined (Fig. 1K). Consistent with our earlier findings, rates of social investigation and USV production significantly increased following 3 days of social isolation (Fig. 1G, I; one-way ANOVAs with repeated measures; $p < 0.05$ for day 0 vs. day 3 in both groups for both behaviors). Following re-group-housing, time spent in social investigation and rates of USV production tended to decrease to pre-isolation levels (Fig. 1G, I, top plots; $p = 0.06$ for day 0 vs. day 17 investigation time and day 0 vs. day 17 total USVs in re-group-housed females). In contrast, females that were single-housed for 14 days continued to spend increased time in social investigation (Fig. 1G, bottom plot; $p < 0.05$ for day 0 vs. day 3 investigation and for day 0 vs. day 17 investigation), and pairs containing 14-day single-housed residents continued to produce elevated rates of USVs (Fig. 1I, bottom plot; $p < 0.05$ for day 0 vs. day 3 USVs and for day 0 vs. day 17 USVs). Time spent mounting tended to follow the same trends as rates of social investigation and USV production in re-group-housed and 14-day single-housed females (Fig. 1H). Along with the attenuation of female social behaviors following re-group-housing, we also found that POA Fos expression was significantly lower in re-group-housed females relative to 14-day single-housed females (Fig. 1K; t-test, $p < 0.001$). These findings support the idea that changes in female social behavior following short-term isolation are reversible and are accompanied by decreased POA Fos expression. Hereinafter, we refer to the population of POA neurons that increase Fos expression in single-housed females that have engaged in same-sex interactions as POA_{iso} neurons, and we next conducted experiments to test whether functional manipulations of POA_{iso} neuronal activity impact the effects of short-term isolation on female social behavior.

Chemogenetic inhibition of POA_{iso} neurons attenuates the effects of social isolation on female social investigation and USV production

If increased activity of POA_{iso} neurons contributes to the effects of short-term isolation on female social behavior, one prediction is that reducing the activity of POA_{iso}

neurons in single-housed females will attenuate the effects of isolation on female social behavior. To test this idea, we employed the TRAP2 activity-dependent labeling strategy to chemogenetically silence POA_{iso} neurons in single-housed females during social interactions with novel, group-housed female visitors (Fig. 2A). Briefly, the POA of TRAP2 female mice was injected bilaterally with a virus driving the Cre-dependent expression of the inhibitory DREADDs receptor hM4Di. Three weeks later, females were single-housed for 3 days and then given a 30-minute social encounter with a novel, group-housed female visitor in their home cage. Following the social interaction, resident females were given an I.P. injection of 4-hydroxytamoxifen (4-OHT), which drives the transient expression of Cre recombinase in recently active neurons and thereby enables the expression of hM4Di in POA_{iso} neurons. Subject females remained single-housed for an additional 24 hours and then were re-group-housed with siblings for 2 weeks. Subject females were then single-housed a second time for 3 days and subsequently given a 30-minute same-sex interaction following I.P. injection of either saline (control) or clozapine-n-oxide (CNO) (saline and CNO tests were run 3 days apart, and the order was counterbalanced across experiments).

Comparison of the social behaviors of single-housed females between CNO and saline sessions revealed that chemogenetic silencing of POA_{iso} neurons significantly reduced resident-initiated investigation (Fig. 2B; N = 12; red points; two-way ANOVA with repeated measures on one factor; $p < 0.01$). Inhibition of POA_{iso} neurons also tended to reduce mounting, although this effect was not statistically significant (Fig. 2D; Kruskal Wallis test performed on difference in mounting time (CNO-saline) for each group; $p > 0.05$). Finally, inhibition of POA_{iso} neurons significantly reduced USV production (Fig. 2D; two-way ANOVA with repeated measures on one factor; $p < 0.01$). In contrast, CNO treatment did not affect the production of any of these social behaviors in single-housed females with GFP expressed in POA_{iso} neurons (Fig. 2B-D; N = 14; black points; $p > 0.05$ for all CNO vs. saline comparisons in the POA_{iso} FLEX-GFP control group). To investigate the specificity of these effects to chemogenetic silencing of POA_{iso} neurons, we also performed control experiments in which activity-dependent chemogenetic silencing was performed caudal to the POA within the anterior hypothalamus (AH) (Figs. 2B-D; N = 12; brown points) or within the VMH (Fig. 2B-D; N = 5; gray points). No significant effects of CNO treatment on resident-initiated investigation, mounting, or USV rate were observed in these control groups (Figs. 2C-D; $p > 0.05$ for all). The effect of chemogenetic inhibition of POA_{iso} neurons to decrease female social behavior also cannot be attributed to an overall decrease in movement (Fig. 2E; $p > 0.5$ for difference in movement between saline and CNO sessions; see Methods). In summary, we demonstrate that chemogenetic silencing of POA_{iso} neurons attenuates isolation-induced changes in social behavior in female mice.

Ablation of POA_{iso} neurons attenuates the effects of social isolation on female mounting

In previous work investigating the role of the POA in regulating rodent social behaviors, studies have reported different effects on behaviors according to whether they employed reversible or irreversible neuronal silencing strategies. Studies that used chemogenetic or optogenetic methods to reversibly silence genetically-defined subsets of POA neurons report decreases in both USV production in males (Chen et al., 2021; Karigo et al., 2021) and in mounting in males and females during interactions with female social partners (Gao et al., 2019; Karigo et al., 2021). In contrast, studies employing caspase-mediated ablation of genetically-defined subsets of POA neurons (Gao et al., 2019; Wei et al., 2018) or electrolytic lesions of the POA (Bean et al., 1981) report decreased mounting but no effects on rates of USV production. To test whether permanent ablation of POA_{iso} neurons attenuates the effects of social isolation on female behavior in a manner similar to the effects of chemogenetic inhibition, we used the TRAP2 activity-dependent labeling strategy to express caspase in and to thereby ablate POA_{iso} neurons (Fig. 3A; see Methods). Vocal and non-vocal social behaviors of resident females were compared pre- and post-ablation, and the same measurements were made in control females expressing GFP in POA_{iso} neurons.

In contrast to the effects of chemogenetic inhibition of POA_{iso} neurons, we found that caspase-mediated ablation of POA_{iso} neurons did not affect rates of social investigation in single-housed females, although both experimental and control females spent more time investigating visitors in the post-4-OHT session (Fig. 3B; two-way ANOVA with repeated measures on one factor; $p > 0.05$ for main effect of group, $p < 0.01$ for main effect of time, $p > 0.05$ for interaction effect). Ablation of POA_{iso} neurons also failed to reduce USV production in pairs containing single-housed females (Fig. 3D; two-way ANOVA with repeated measures on one factor; $p > 0.05$ for pre-4-OHT vs. post-4-OHT USV rates in POA_{iso}-caspase females). Notably, ablation of POA_{iso} neurons significantly reduced mounting in single-housed females (Fig. 3C; Mann Whitney U test performed on the difference in mounting time (post-4-OHT - pre-4-OHT, $p = 0.01$). Taken together with our chemogenetic inhibition data, these results show that both reversible inhibition or irreversible ablation of POA_{iso} neurons in single-housed female mice attenuates the effects of short-term isolation on mounting behavior, whereas only chemogenetic inhibition of POA_{iso} neurons attenuates the effects of short-term isolation on female social investigation and USV production.

Optogenetic activation of POA_{iso} neurons elicits USV production

To understand whether artificial activation of POA_{iso} neurons can recapitulate the effects of short-term isolation on female social behavior, we assessed the effects of optogenetic activation of POA_{iso} neurons on the social behaviors of group-housed females. The TRAP2 strategy was used to express either channelrhodopsin (ChR2) or GFP in POA_{iso} neurons (Fig. 4A; see Methods), and females were re-group-housed for two weeks before beginning optogenetic activation experiments. The effects of optogenetically activating POA_{iso} neurons were first assessed for each subject female in a 5-minute solo session, in which the female was tested alone in a behavior chamber while pulses of blue light were delivered unilaterally to the POA (473 nm, 10 mW, 20-50 Hz, 10-20 ms pulses, 5-10s train durations). The effects of optogenetically activating POA_{iso} neurons were then assessed for each subject female in a 20-minute social session, in which a novel, group-housed female visitor was added to the behavior chamber. The pair was allowed to interact in the absence of optogenetic stimulation for the first and last 5 minutes of the social session, and pulses of blue light were delivered to the POA of the subject female throughout the middle 10 minutes of the session (Fig. 4A).

When POA_{iso}-ChR2 females were tested alone, we found that optogenetic activation of POA_{iso} neurons elicited weak-to-moderate USV production in 4 of 8 females, but the comparison of USV rates from pre-laser baseline to the laser stimulation period was not significant at the level of the entire group (Fig. 4B; Mann Whitney U test performed on the difference in USV rates (laser - pre-laser), $p = 0.09$). In POA_{iso}-GFP control females, laser stimulation failed to elicit USV production (0 ± 0 USVs elicited in $N = 6$ POA_{iso}-GFP controls). Interestingly, we found that when laser stimulation was applied during social sessions, optogenetic activation of POA_{iso} neurons more readily elicited USV production than in solo sessions (Fig. 4C; USVs elicited by blue laser stimulation in 7 of 8 POA_{iso}-ChR2 females; Mann Whitney U test performed on the difference in USV rates (laser - pre-laser), $p = 0.006$). Moreover, optogenetic activation elicited higher rates of USVs when applied at times when subject females were in close proximity to visitor females (within 2 mouse body lengths) as compared to times when the females were farther apart (mean increase in USV rates from pre-laser to laser period was 2.96 ± 2.32 USVs/s for “near” stimulations, 1.84 ± 1.75 USVs/s for “far” stimulations; paired t-test performed on the difference in USV rates (laser - pre-laser) for “far” vs. “near” stimulations; $p = 0.02$). In summary, optogenetic activation of POA_{iso} neurons elicits USV production in group-housed females, and the efficacy of this effect is modulated by social context and proximity to a social partner.

In contrast to the effects on USV production, optogenetic activation of POA_{iso} neurons failed to extend the duration of social investigation bouts (paired t-test performed on mean duration of social investigation bouts for each POA_{iso}-ChR2 female that overlapped

with laser stimulation vs. those that did not; $p > 0.05$). Moreover, optogenetic activation of POA_{iso} neurons only infrequently elicited mounting (activation elicited n =1 bout of mounting in N = 1 POA_{iso}-ChR2 female, n = 2 bouts of mounting in N = 1 POA_{iso}-ChR2 female, and n = 0 bouts of mounting in the remaining N = 7 POA_{iso}-ChR2 females). In summary, optogenetic activation of POA_{iso} neurons elicits USV production from group-housed females, particularly when female subjects are engaged in interactions with female visitors, but otherwise fails to recapitulate the effects of short-term isolation on the social behaviors of female mice.

Previous studies have found that USV production can be elicited in female and male mice by artificial activation of $VGAT^+$ POA neurons (Gao et al., 2019), $Esr1^+$ POA neurons (which are predominantly $VGAT^+$) (Chen et al., 2021; Michael et al., 2020), as well as POA neurons that send axonal projections to the caudolateral PAG (which are predominantly $VGAT^+$) (Chen et al., 2021; Michael et al., 2020). To ask to what extent POA_{iso} neurons overlap with these previously described populations, we first evaluated the neurotransmitter phenotype of POA_{iso} neurons by performing two-color in situ hybridization for c-fos mRNA and vesicular GABA transporter (VGAT) mRNA and calculating the percentage of Fos^+ POA neurons that co-expressed VGAT. This analysis revealed that a majority of POA_{iso} neurons are GABAergic (Fig. S2A-B; N = 4, 76 ± 8.8%). We next used the TRAP2 activity-dependent labeling strategy to express GFP in POA_{iso} neurons and found GFP-positive axons within the caudolateral PAG, indicating that at least some POA_{iso} neurons send axonal projections to the PAG (Fig. S2C-D; see Methods). Finally, we combined retrograde tracing from the caudolateral PAG with Fos immunostaining to quantify the percentage of PAG-projecting POA neurons that increase Fos expression in single-housed females following same-sex interactions. This experiment revealed that around 20% of PAG-projecting POA neurons express Fos in single-housed females following same-sex interactions (Fig. S2E-F; N = 4 females, percentage of tdTomato neurons that are Fos-positive = 18.3 ± 2.9%). These findings suggest that a subset of POA_{iso} neurons overlap with GABAergic, PAG-projecting POA neurons that have been demonstrated in previous work to promote USVs via disinhibition of excitatory PAG neurons important to USV production (Chen et al., 2021; Michael et al., 2020).

POA neurons increase their activity in single-housed male mice following opposite-sex but not same-sex social interactions

Given our findings that POA_{iso} neurons contribute to isolation-induced changes in the social behaviors of female mice, we next wondered whether a similar population of POA neurons contributes to isolation-induced changes in social behavior in male mice. To address these questions, we measured the vocal and non-vocal social behaviors of sexually naïve males, which were either group-housed with same-sex siblings or single-housed for

three days and then given a 30-minute social interaction with a novel, group-housed visitor. To consider the effects of isolation on male social behavior in different social contexts, males were given either a social encounter with a same-sex visitor (MM context) or with an opposite-sex visitor (MF context). Following these social interaction tests, we collected the brains of the subject males and performed immunostaining to measure Fos expression within the POA. Consistent with our prior work (Zhao et al., 2021), we found that males exhibit higher rates of social investigation, higher rates of mounting, and produce more USVs during interactions with females than during same-sex interactions (Fig. 5A-C; $p < 0.05$ for main effect of social context for all three behaviors). With respect to resident-initiated investigation, we found a significant main effect of housing, indicating that single-housed males spent more time investigating visitors during both opposite-sex and same-sex interactions (Fig. 5A; two-way ANOVA, $p = 0.02$ for main effect of housing). In contrast, single-housed males spent more time mounting female visitors than did group-housed males, but there were no differences in mounting between single-housed and group-housed males during same-sex interactions (Fig. 5B; two-way ANOVA, $p < 0.05$ for difference between single-housed males interacting with females and all other groups). Similarly, there was also a context-dependent effect of social isolation on male USV production, whereby only single-housed males that interacted with female visitors exhibited increased USV production relative to group-housed males (Fig. 5C; two-way ANOVA with post-hoc Tukey's HSD tests; $p < 0.001$ for total USVs in single-housed MF vs. group-housed MF trials; $p > 0.05$ for total USVs in single-housed MM vs. group-housed MM trials). The finding that short-term isolation exerts larger effects on male social behavior during subsequent opposite-sex interactions relative to same-sex interactions is consistent with prior work (Zhao et al., 2021). When we examined POA Fos expression in these four groups of males, we found that POA Fos was significantly elevated in single-housed males following interactions with females relative to the other three groups (Fig. 5D; two-way ANOVA, Tukey's post-hoc HSD tests; $p < 0.05$ for difference in POA Fos between single-housed MF and all other groups). In summary, the effects of short-term isolation on male social behavior are context-dependent, and increased Fos expression within the POA is seen in single-housed males following interactions with females, a context marked by increased male social investigation, increased male mounting, and increased male USV production.

To test whether neural activity in male POA_{iso} neurons contributes to isolation-induced changes in male social behavior, we used the TRAP2 strategy to chemogenetically silence POA_{iso} neurons in single-housed males during social interactions with novel, group-housed females (see Methods). The vocal and non-vocal behaviors of subject males were measured and compared during 30-minute social interactions following I.P. injection of either

saline or CNO. Control males were treated identically but were injected with a virus to drive expression of GFP in POA_{iso} neurons. In contrast to our findings in females, chemogenetic inhibition of male POA_{iso} neurons tended to reduce time spent mounting (Fig. 5G; Mann Whitney U test performed on difference in mounting time (CNO - saline); $p = 0.13$ for difference between groups) but did not change rates of resident-initiated social investigation (Fig. 5F; two-way ANOVA with repeated measures on one factor; $p = 0.01$ for main effect of group; $p > 0.05$ for main effect of drug and for interaction effect) and also did not affect USV rates (Fig. 5H; two-way ANOVA with repeated measures on one factor; $p > 0.05$ for main effects and interaction effect). In summary, we find that chemogenetic silencing of male POA_{iso} neurons tends to reduce mounting during subsequent social interactions with females but does not reduce social investigation or USV production, a pattern of results that differs from the effects on single-housed female social behavior of chemogenetically silencing female POA_{iso} neurons.

Discussion

In the current study, we identify and characterize a population of preoptic hypothalamic neurons that contribute to the effects of short-term social isolation on the social behaviors of mice. These POA_{iso} neurons exhibit increased Fos expression in single-housed female mice following same-sex social interactions, and this increase in Fos expression scales positively with the time females spend investigating and mounting female visitors and tends also to scale with rates of USVs. Chemogenetic silencing of POA_{iso} neurons attenuates the effects of social isolation on female social behavior, significantly reducing social investigation and USV production while tending to reduce mounting. In contrast, irreversible ablation of POA_{iso} neurons significantly reduces mounting in single-housed females but has no effect on rates of social investigation or USVs. Optogenetic activation of POA_{iso} neurons partially recapitulates the effects of short-term isolation on female behavior and promotes USV production in female mice, particularly during same-sex social interactions and when in close proximity to female visitors. Finally, we extended our analyses to male mice to understand whether similar POA neurons may mediate changes in male social behavior following short-term isolation. We find that short-term isolation exerts more robust effects on male behavior during subsequent interactions with females than during subsequent interactions with males, and increased POA Fos expression is only seen in single-housed males following social interactions with females. Interestingly, chemogenetic silencing of these POA_{iso} neurons tends to reduce mounting but has no effect on social investigation and USV production, in contrast to the effects of chemogenetically silencing POA_{iso} neurons in females. Together, these experiments identify a population of

preoptic hypothalamic neurons that promote social behaviors in single-housed mice in a manner that depends on sex and social context.

An extensive body of past work has implicated the POA in the regulation of male sexual behavior, including in the regulation of male courtship vocalizations in both rodents and birds (Alger and Riters, 2006; Bean et al., 1981; Gao et al., 2019; Merari and Ginton, 1975; Riters, 2012; Riters et al., 2000; Riters and Ball, 1999; Wei et al., 2018). Past work has also shown that activation of genetically-defined subsets of POA can elicit the production of USVs in both male and female mice (Chen et al., 2021; Gao et al., 2019; Karigo et al., 2021; Michael et al., 2020). However, whether the POA regulates natural USV production in female mice remained unclear. In the current study, we demonstrate that reversible silencing of POA neurons that increase their activity during same-sex interactions decreases female USV production, indicating that the POA regulates the production of USVs by single-housed females engaged in same-sex interactions. Whether these same neurons regulate female USV production in other behavioral contexts, including in group-housed females and in females interacting with male partners, remains an important open question. In addition to attenuating USV production, we found that silencing of POA_{iso} neurons in single-housed females significantly reduced social investigation of a same-sex partner and also tended to reduce mounting. Our retrograde and anterograde tracing experiments demonstrate that at least a subset of POA_{iso} neurons project to the caudolateral PAG where neurons important for USV production reside, and an attractive possibility is that POA_{iso} neurons promote USV production via disinhibition of PAG-USV neurons as previously demonstrated for genetically-defined subsets of POA neurons (Chen et al., 2021; Michael et al., 2020; Tschida et al., 2019). Future experiments will be required to determine whether PAG-projecting POA_{iso} neurons also regulate social investigation and mounting, or alternatively, whether distinct molecularly-defined or projection-defined subsets of POA_{iso} neurons differentially regulate these different aspects of female social behavior. The latter organization would be reminiscent of how projection-defined subsets of galanin-expressing POA neurons regulate different aspects of parental behavior (Kohl et al., 2018).

Although reversible inhibition of POA_{iso} neurons reduced both social investigation and USV production in single-housed females, permanent caspase-mediated ablation of these neurons significantly reduced mounting but had no effects on social investigation or USV production. These differences are largely consistent with prior studies that reported effects on both mounting and USV production following reversible manipulations of POA activity and effects on mounting but not on USV production following irreversible manipulations of POA activity (Bean et al., 1981; Chen et al., 2021; Gao et al., 2019; Karigo et al., 2021; Wei et al.,

2018). One possibility is that POA_{iso} neurons do not directly regulate USV production but rather that reversible silencing of these neurons causes off-target disruptions of neural activity in interconnected brain regions that in turn directly regulate USV production. Such a relationship was demonstrated for motor cortex, whereby reversible silencing of motor cortex disrupted performance of a learned forelimb reaching task in rats, while permanent lesions of motor cortex had no effect on task performance after learning (Otchy et al., 2015). However, our finding that optogenetic activation of POA_{iso} neurons elicits USV production, along with past work demonstrating that POA activation elicits USV production (Chen et al., 2021; Gao et al., 2019; Karigo et al., 2021; Michael et al., 2020) supports the idea that the POA directly regulates USV production. An alternative explanation for the apparently contradictory effects of chemogenetic silencing vs. ablation of POA_{iso} neurons is that while the POA plays an obligatory role in mounting behavior (at least in certain contexts, see below), compensatory changes in additional, non-POA circuits that promote USV production (and social investigation) are sufficient to compensate for the permanent loss of POA_{iso} neurons, leaving these behaviors unperturbed following POA_{iso} neuronal ablation. The identification of forebrain-to-midbrain circuits that regulate USV production in both females and males remains an important future goal.

Our finding that POA_{iso} neurons regulate female-female mounting extends recent work examining the role of hypothalamic regions in regulating male mounting behavior in different social contexts (Karigo et al., 2021). Although the POA plays a well-established role in the regulation of mounting behavior by male rodents during interactions with females, interactions which are typically marked by high rates of USV production and are considered affiliative, the authors found that the VMH regulates male mounting behavior during interactions with other males, which is typically not accompanied by USV production and often precedes fighting. Taken together with the findings of the current study, we conclude that the POA regulates mounting behavior in both male and female mice that is directed toward female social partners and is accompanied by USV production. The question of whether the social behaviors exhibited by single-housed female mice during same-sex interactions are indeed affiliative and how these behaviors shape future interactions with female social partners are important questions that remain to be addressed. Although chemogenetic silencing of POA_{iso} neurons tended to reduce female mounting and ablation of POA_{iso} neurons significantly reduced female mounting, we were not able to reliably elicit mounting behavior through optogenetic activation of POA_{iso} neurons (optogenetically-elicited mounting was observed in n = 3 laser stimulations across N = 2 POA_{iso}-ChR2 females). We note that previous studies that elicited mounting in male mice via optogenetic activation of either $Esr1^{+}$ POA neurons or POA neurons that co-express Esr1 and VGAT used longer

laser stimulation trains (15-30s) than we employed in the current study (Karigo et al., 2021; Wei et al., 2018). It is possible that longer periods of optogenetic activation of POA_{iso} neurons would be more effective in eliciting mounting in group-housed females, and another possibility is that POA_{iso} neurons overlap somewhat but not perfectly with the genetically-defined groups of POA neurons manipulated in those prior studies. Regardless, our finding that optogenetic activation of POA_{iso} neurons promotes USV production efficaciously relative to mounting indicates that effects on USV production are not secondary to effects on other female social behaviors.

To understand whether a similar population of POA neurons might regulate changes in social behavior following short-term isolation in males, we extended our experiments to single-housed males that subsequently interacted with either a male social partner or with a female social partner. Consistent with our prior work (Zhao et al., 2021), we found that short-term isolation exerts more robust on the effects of male behavior during subsequent interactions with females than during interactions with males. Although single-housed males exhibited increased rates of social investigation while interacting with both males and females relative to group-housed males, single-housed males that interacted with females exhibited increases in all measured social behaviors (social investigation, USV production, and mounting), a pattern of behavioral changes that is similar to what we observed in single-housed females. We also observed that a population of POA neurons increased Fos expression in single-housed males following interactions with female visitors but not following interactions with male visitors. Unexpectedly, we found that the effects of chemogenetically inhibiting POA_{iso} neurons in males differed from those in females. Namely, while reversible inhibition of POA_{iso} neurons tended to reduce mounting during interactions between single-housed subject males and female visitors, there were no effects on rates of social investigation and USV production. These findings differ also from recent work showing that chemogenetic inhibition (Chen et al., 2021) or optogenetic inhibition (Karigo et al., 2021) of $Esr1^{+}$ POA neurons reduces USV production in male mice. Although the factors that account for this difference in results are unclear, one possibility is that our TRAP2-based viral labeling in males is biased toward POA neurons that regulate mounting as compared to POA neurons that regulate USV production, although as stated above, more work is required to understand whether these different social behaviors are regulated by distinct or overlapping subsets of POA neurons. Future experiments can also explore to what extent female and male POA_{iso} neurons represent molecularly, anatomically, and functionally similar or dissimilar neuronal populations.

The current study adds to an emerging body of literature implicating the POA in the regulation of social behavior in both females and males, including in non-sexual social contexts (Fukumitsu et al., 2022; Hu et al., 2021; Liu et al., 2023; McHenry et al., 2017; Wu et al., 2021). Our findings also complement recent work that has described a role for the POA in regulating behavioral responses to social isolation in female mice. A recent study using BALB/c mice found that reunion with same-sex cagemates following short-term "somatic isolation" (i.e., separation from cagemates via a partition that permits visual, auditory, and olfactory signaling but prevents physical contact) increases the activity of calcitonin-receptor (Calcr) expressing POA neurons (Fukumitsu et al., 2023). Knockdown of Calcr expression in these neurons reduced social-seeking behaviors directed at the cage partition exhibited by single-housed females, and chemogenetic activation of these neurons increased partition-biting behavior in single-housed females. Another recent study using female FVB/NJ mice applied a TRAP2-based intersectional approach to identify POA neurons that increase their activity following reunion with same-sex cagemates ($MPN_{reunion}$ neurons) (Liu et al., 2023). Optogenetic activation of these neurons did not alter social investigation in group-housed females, whereas activation of these neurons during reunion with cagemates following short-term social isolation decreased social investigation. However, optogenetic inhibition of $MPN_{reunion}$ during reunion did not alter rates of social investigation in single-housed females. Although we did not test the effects of activating POA_{iso} neurons in single-housed females in the current study, the difference in the effects of inhibiting POA_{iso} neurons on the behavior of single-housed females (reduced rates of social investigation, USV production, and mounting) relative to the effects of optogenetic inhibition of $MPN_{reunion}$ neurons in Liu et al. (no effect on social investigation during reunion) suggest that these may represent distinct populations of POA neurons. We note that in the current study, single-housed female subjects remained single-housed for 24 hours following social interaction TRAPing sessions, a design intended to maximize viral labeling of POA neurons that promote increased female social behaviors and that would likely in turn minimize viral labeling of POA neurons that promote social satiety. Taken together, these studies highlight a complex role for the POA in regulating multiple aspects of changes in social behavior following short-term social isolation. Although some studies of social isolation have avoided the use of C57BL/6J female mice, the robust triad of changes in social behavior exhibited by these females following short-term isolation affords a powerful opportunity to continue investigating neural circuit mechanisms through which short-term social isolation promotes social behaviors, as well as to investigate how hypothalamic circuits regulate the coordinated production of suites of social behaviors during female-female social interactions.

Acknowledgements: Thanks to Frank Drank and other CARE staff for their excellent mouse husbandry. All experimental design schematics included in the figures were created with Biorender.com.

Author contributions: X.Z. and K.A.T. designed the experiments. X.Z. and Y.C. conducted the experiments. X.Z., Y.C., D.S., V.C., D.D., J.W.S., A.S., and K.A.T. analyzed data. X.Z. and K.A.T. wrote the manuscript, and all authors approved the final version.

Declaration of Interests: The authors declare no competing interests.

Figure legends

Figure 1. The POA contains neurons that increase Fos expression in single-housed females following same-sex interactions. (A) Schematic of experiment to measure Fos expression in group-housed and single-housed females following same-sex social interactions. (B) Total time spent engaged in resident-initiated social investigation for group-housed residents (teal) and single-housed residents (maroon). (C) Same as (B), for total resident-initiated mounting time. (D) Same as (B), for total USVs recorded from pairs containing group-housed or single-housed residents. (E) Left-most image shows the location of the POA in a coronal brain section. Representative confocal images show Fos expression (green) in the POA of a group-housed female (left) and a single-housed female (right) following same-sex social interactions. Blue, Neurotrace. (F) Quantification of Fos-positive neurons is shown for the POA (left), the VMH (middle), and the caudolateral PAG (right) for group-housed and single-housed females. Open bars show data from females that did not engage in social interactions with novel females (baseline), and closed bars show data from females following social interactions with novel females (interaction). (G) Total time spent in resident-initiated interaction is plotted for 14-day single-housed (maroon) and re-group-housed females (teal) during same-sex interactions that occurred prior to isolation (day 0), following 3 days of isolation (day 3), and on the test day (day 17). (H) Same as (G), for total resident-initiated mounting time. (I) Same as (G), for total USVs. (J) Quantification of Fos-positive POA neurons is shown for 14-day single-housed females (maroon) and re-group-housed females (teal).

Figure 2. Effects of chemogenetic inhibition of POA_{iso} neurons on the social behaviors of single-housed female mice. (A) Experimental timeline and viral strategy to chemogenetically inhibit the activity of POA_{iso} neurons in single-housed females. (B) Total time spent in resident-initiated social investigation is shown on saline and CNO days for 4 experimental groups: (red symbols) experimental females in which hM4Di is expressed in POA_{iso} neurons; (black symbols) control females in which GFP is expressed in POA_{iso} neurons; (brown symbols) control females in which hM4Di is expressed in 'TRAPed' AH neurons; (gray symbols) control females in which hM4Di is expressed in 'TRAPed' VMH neurons. (C) Same as (B), for total duration of resident-initiated mounting. (D) Same as (B), for total USVs. (E) Total movement is plotted for females with hM4Di expressed in POA_{iso} neurons, on saline days vs. CNO days.

Figure 3. Effects of caspase-mediated ablation of POA_{iso} neurons on the social behaviors of single-housed female mice. (A) Experimental timeline and viral strategy for caspase-mediated ablation of POA_{iso} neurons in single-housed females. (B) Total time spent

in resident-initiated social investigation is shown pre- and post-4-OHT treatment for 2 experimental groups: (red symbols) experimental females in which caspase is expressed in POA_{iso} neurons; (black symbols) control females in which GFP is expressed in POA_{iso} neurons. (C) Same as (B), for total duration of resident-initiated mounting. (D) Same as (B), for total USVs.

Figure 4. Effects of optogenetic activation of POA_{iso} neurons on the behaviors of group-housed female mice. (A) Experimental timeline and viral strategy to optogenetically activate POA_{iso} neurons in group-housed females. (B) Mean total USVs produced during social sessions shown for pre-laser periods and during laser stimulation periods for experimental females with ChR2 expressed in POA_{iso} neurons (red symbols; N = 9) and for control females with GFP expressed in POA_{iso} neurons (black symbols, N = 6). (C) Same as (B), for social sessions. (D) Spectrograms are shown from a representative POA_{iso}-ChR2 female to illustrate USVs that were elicited through optogenetic activation of POA_{iso} neurons in a solo session (top) and a social session (bottom). Blue bars indicate timing of laser stimulation.

Figure 5. Context-dependent differences in POA Fos expression and effects of chemogenetic inhibition of POA_{iso} neurons on the social behaviors of single-housed male mice. (A) Total time spent in resident-initiated social investigation is shown for group-housed male residents (teal) and single-housed male residents (maroon) during interactions with either female visitors (left) or male visitors (right). (B) Same as (A), for total resident-initiated mounting time. (C) Same as (A), for total USVs recorded from pairs containing group-housed or single-housed male residents. (D) Total number of Fos-positive POA neurons is shown for group-housed male residents (teal) and single-housed male residents (maroon) following interactions with female visitors (left) or male visitors (right). (E) Experimental timeline and viral strategy to chemogenetically inhibit the activity of POA_{iso} neurons in single-housed males. (F) Total time spent in resident-initiated social investigation is shown on saline and CNO days for experimental males in which hM4Di is expressed in POA_{iso} neurons (red symbols, N = 7) and control males in which GFP is expressed in POA_{iso} neurons (black symbols, N = 7). (G) Same as (F), for total duration of resident-initiated mounting. (H) Same as (F), for total USVs.

Materials and methods

Key Resources

REAGENT or RESOURCE	SOURCE	IDENTIFIER
Antibodies		
c-Fos (9F6) Rabbit mAb	Cell Signaling Technology	2250S
Alexa Fluor 488 goat-anti-rabbit	Invitrogen	A-11008
Neurotrace 435/455 Blue	Thermo Fischer Scientific	CAT#: N21479
Commercial assay or kit		
HCR v3.0	Molecular Instruments	
Bacterial and Virus Strains		
AAV2/1-hSyn-FLEX-hM4Di-mCherry	Addgene	RRID: Addgene_44262
AAV2/1-Ef1alpha-hChR2(h134R)-EYFP-WPRE-HGHpA	Addgene	RRID: Addgene_20298
AAVrg-pgk-Cre	Addgene	RRID: Addgene_24593
pAAV-flex-taCasp3-TEVp	Addgene	RRID: Addgene_45580
AAV2/1-pCAG-FLEX-EGFP-WPRE	Addgene	RRID: Addgene_51502
Chemicals, Peptides, and Recombinant Proteins		
Clozapine N-oxide dihydrochloride	Hello Bio	HB6149; E1458-2-1
4-Hydroxytamoxifen	Hello Bio	HB6040
Experimental Models: Organisms/Strains		
TRAP2 Fos$^{tm2.1(icre/ERT2)Luo}$/J	Jackson Labs	IMSR_JAX:030323
Ai14 B6.Cg*Gt(ROSA)26Sor*$^{tm14(CAG-tdTomato)Hze}$/J	Jackson Labs	IMSR_JAX:007914
C57BL/6J	Jackson Labs	IMSR_JAX:000664
Software and Algorithms		
MATLAB	Mathworks	http://www.mathworks.com RRID: SCR_001622
ZEN	Zeiss	https://www.zeiss.com RRID:SCR_013672
Spike2	CED	http://ced.co.uk RRID:SCR_000903
ImageJ	NIH	https://imagej.net/ij/ RRID:SCR_003070
Behavioral Observation Research Interactive Software	Open Behavior	https://github.com/olivierfriard/BORIS RRID:SCR_021509
R Project for Statistical Computing	R Core Team	http://www.r-project.org/ RRID:SCR_001905
R Studio	Posit	https://posit.co/ RRID:SCR_000432

Lead contact

Further information and requests for resources should be directed to and will be fulfilled by the lead contact, Katherine Tschida (kat227@cornell.edu).

Experimental models and subject details

Animal statement

All experiments and procedures were conducted according to protocols approved by the Cornell University Institutional Animal Care and Use Committee (protocol #2020-001).

Animals

TRAP2 (Jackson Laboratories, 030323) and Ai14 (Jackson Laboratories, 007914) mice were at least 8 weeks old at the time of the experiments or surgeries. TRAP2;Ai14 mice were generated by crossing TRAP2 with Ai14. All mice were kept on a 12:12 reversed light/dark cycle, were housed in ventilated micro-isolator cages in a controlled environment with regulated temperature and humidity, and were provided with unrestricted access to food and water. A running wheel (Innovive) was present in all homecages from the time of weaning and was subsequently removed immediately before initiating the social interaction test. Mouse cages were cleaned weekly, and experiments were never conducted on cage change days.

Methods details

Social isolation and social interaction tests

Female and male subject mice were either group-housed with same-sex siblings or separated from their cage mates and individually housed in clean cages for three days prior to behavioral tests. In the case of group-housed subject mice, siblings were temporarily removed from the home cage for the duration of the test. The subject animal's home cage was then placed in a sound-attenuating recording chamber (Med Associates) equipped with an ultrasonic microphone (Avisoft), an infrared light source (Tendelux), and a webcam (Logitech, with the infrared filter removed to enable video recording under infrared lighting conditions). A novel, group-housed visitor mouse (female or male mouse on a C57BL/6 background) was placed in the home cage of the subject mouse, and vocal and non-vocal behaviors were recorded for 30 minutes. Visitor mice were used across multiple experiments (< 6 in total), including in interactions with both group-housed and single-housed subject mice. Visitor females used in male-female interactions were never used for female-female experiments, but a subset of visitors used in female-female interactions were subsequently used in male-female experiments.

A separate cohort of female mice was used to investigate the effects on social behavior of re-group-housing following a period of social isolation. For this cohort of mice, social

interaction tests with novel, group-housed female visitors were conducted at three timepoints: (1) on day 0, when subject females were still group-housed; (2) On day 3, after being single-housed for 3 days; (3) on day 17, after a randomly selected subset of subject females were re-group-housed with their siblings for two weeks, and the remaining female subjects remained single-housed for two weeks.

USV recording and detection

USVs were recorded with an ultrasonic microphone (Avisoft, CMPA/CM16), amplified (Presonus TubePreV2), and digitized at 250 kHz (Avisoft UltrasoundGate 166H or CED Power 1401). USVs were detected with custom MATLAB codes (Tschida et al., 2019) using the following parameters (mean frequency > 45 kHz; spectral purity > 0.3; spectral discontinuity < 1.00; minimum USV duration = 5 ms; minimum inter-syllable interval = 30 ms).

Analyses of non-vocal social behaviors

Trained observers used BORIS software (v.8.13; Friard and Gamba, 2016) to score the following non-vocal behaviors: resident-initiated social investigation and resident-initiated mounting. Social investigation included sniffing and following. Resident-initiated mounting of the visitor typically occurred following a period of resident-initiated social investigation, with the resident mouse positioning its forelimbs on top of the body of the visitor, sometimes with pelvic thrusts and sometimes without. Neither visitor-initiated mounting nor fighting were observed in our dataset.

In some trials, total movement was estimated using a custom MATLAB code that allows the user to mark the position of a mouse in every 30th frame (i.e., once per second). Total movement was then calculated as the sum of changes in position across pairs of marked frames.

Fos immunohistochemistry

Two hours following the start of the social interaction test, mice were deeply anesthetized using isoflurane and then transcardially perfused with phosphate-buffered saline (PBS, pH 7.4), followed by 4% paraformaldehyde (PFA; Sigma-Aldrich, in 0.1 M PBS, pH 7.4). Brains were subsequently dissected and post-fixed in 4% PFA for 24 hours at 4°C, followed by immersion in 30% sucrose solution in PBS for 48 hours at 4°C. Afterward, brains were embedded in frozen section embedding medium (Surgipath, VWR), flash frozen in a dry ice-ethanol (100%) bath, and then stored at –80°C until sectioning. Sections were cut on a cryostat (Leica CM1950) to a thickness of 80 µm, washed in PBS (3 x 5 mins at RT),

permeabilized for 2-3 hours in PBS containing 1% Triton X-100 (PBST), and then blocked in 0.3% PBST containing 10% Blocking One (Nacalai USA) for 1 hour at RT on a shaker. Sections were then incubated for 24 hours at 4°C with primary antibody in blocking solution (1:1000 rabbit-anti-Fos, Cell Signaling Technologies, 2250S), washed 3 x 30 minutes in 0.3% PBST, then incubated for 24 hours at 4°C with secondary antibody in blocking solution (1:1000, Alexa Fluor 488 goat-anti-rabbit, Invitrogen, plus 1:500 NeuroTrace, Invitrogen) Finally, sections were washed for 2 x 10 minutes in 0.3% PBST, followed by washing for 2 x 10 minutes in PBS. After mounting on slides, sections were dried and coverslipped with Fluromount G (Southern Biotech). Slides were imaged with a 10x objective on a Zeiss 900 laser scanning confocal microscope, and Fos-positive neurons within regions of interest were counted manually by trained observers.

Floating section two-color in situ hybridization

In situ hybridization was conducted using hybridization chain reaction (HCR v3.0, Molecular Instruments). Ten minutes after the completion of the 30-minute social interaction tests, mice underwent transcardial perfusion with RNase-free PBS (DEPC-treated), followed by 4% PFA. Dissected brain samples were post-fixed overnight in 4% PFA at 4°C, cryoprotected in a 30% sucrose solution in DEPC-PBS at 4°C for 48 hours, flash frozen in section embedding medium, and stored at –80°C until sectioning. 40 µm-thick coronal floating sections were collected into sterile 24-well plates in DEPC-PBS. These sections were briefly fixed once again for 5 minutes in 4% PFA and subsequently immersed in 70% EtOH in DEPC-PBS overnight. Sections were then rinsed in DEPC-PBS, incubated for 45 minutes in 5% SDS in DEPC-PBS, followed by a series of rinses and incubations: 2x SSCT, pre-incubation in HCR hybridization buffer at 37°C, and incubation in HCR hybridization buffer containing RNA probes (VGAT and Fos) overnight at 37°C. Sections were then rinsed 4 x 15 minutes at 37°C in HCR probe wash buffer, rinsed in 2X SSCT, pre-incubated in HCR amplification buffer, and then incubated in HCR amplification buffer containing HCR amplifiers at RT for approximately 48 hours. On the final day, sections were rinsed in 2x SSCT, counterstained with DAPI (Thermo Fisher, 1:5000), rinsed again with 2x SSCT, mounted on slides, and coverslipped with Fluoromount-G (Southern Biotech). After drying, slides were imaged with a 10x or 20x objective on a Zeiss 900 laser scanning microscope. Neurons were scored from three sections of tissue from the POA from each mouse, and the absence of presence of staining for different probes was quantified manually by trained scorers.

Viruses

The following viruses and injection volumes were used: AAV2/1-hSyn-FLEX-hM4Di-mCherry (Addgene #44262, 200 nL), AAV2/1-CAG-FLEX-EGFP-WPRE (Addgene #51502, 200 nL),

AAV2/5-Ef1alpha-FLEX-taCasp3-TEVp (Addgene #45580, 200 nL), AAV2/1-Ef1alpha-hChR2(h134R)-EYFP-WPRE-HGHpA (Addgene #20298, 200 nL), AAVrg-pgk-Cre (Addgene #24593, 200 nL). The final injection coordinates were as follows: POA, AP = -0.1 mm, ML = 0.6 mm, DV = 5.1 mm; AH, AP = -0.7 mm, ML = 0.6 mm, DV = 5.1 mm; VMH, AP = -1.5 mm, ML = 0.7 mm, DV = 5.4 mm; PAG, AP = -4.7 mm, ML = 0.6 mm, DV = 1.75 mm. Viruses were pressure-injected using a pulled glass pipettes mounted in a programmable nanoliter injector (Nanoject III, Drummond) at a rate of 15 nL every 60 s.

Stereotaxic Surgery

Mice were anesthetized using isoflurane (2.5% for induction, then 1.5 - 2.5% for maintenance) and then securely positioned in a stereotaxic apparatus (Angle Two, Leica). A midline incision in the scalp was made to expose the skull, and small craniotomies were created dorsal to each injection site using a surgical drill. Viral injection pipettes were left in place for a minimum of 10 minutes before and after viral injections to minimize backflow upon pipette withdrawal from the brain. Surgical sutures (LOOK 774B, Fisher Scientific) and tissue adhesive (3M) were used to close the incision.

For optogenetic activation experiments, an optogenetic ferrule (RWD Fiber Optic Cannula, Ø1.25 mm Ceramic Ferrule, 200 µm Core, 0.22 NA, L = 7 mm) was implanted approximately 250 µm above the viral injection site immediately following the viral injection and was secured in place with Metabond (Parkell).

TRAP activity-dependent labeling

Solutions of 4-hydroxytamoxifen (4-OHT, HelloBio, HB6040) were prepared by dissolving 4-OHT powder at 20 mg/mL in ethanol by shaking at 37°C, and aliquots (75 uL) were then stored at -20°C. Before use, 4-OHT was redissolved in ethanol by shaking at 37°C and filtered corn oil was added (150 uL). Ethanol was then evaporated by vacuum under centrifugation to give a final concentration of 10 mg/mL, and the 4-OHT solution was used on the same day it was prepared.

To express viral transgenes in recently active neurons, we used the Targeted Recombination in Active Populations (TRAP2) strategy. Two weeks following viral injection, TRAP2 and TRAP2;Ai14 mice were given 30-minute social encounters (as described above). Following the social encounter, subject mice received I.P. injections of 4-OHT (50 mg/kg) to enable expression of viral transgenes in recently active neurons. To minimize neural activity triggered by stimuli outside of the social interaction test, all subject animals

were individually housed for an additional 24 hours following 4-OHT treatment before being re-group-housed with their same-sex siblings.

Chemogenetic inhibition

To reversibly reduce neuronal activity, TRAP2 female mice received bilateral injections of an Cre-dependent inhibitory DREADDs virus into the hypothalamus (AAV2/1-hSyn-FLEX-hM4Di-mCherry; injected into the POA, AH, or VMH) as described above. TRAP2 male mice received the same viral injections into the POA only. Three weeks later, mice were single-housed for 3 days and then were subsequently given a 30-minute social encounter with a novel, group-housed female visitor. Subject mice then received an I.P. injection of 4-OHT to enable expression of hM4Di in activity-defined populations of hypothalamic neurons. Two weeks later, subject mice received an I.P. injection of either sterile saline (as a control) or clozapine-n-oxide (CNO, 4 mg/kg, Hello Bio HB6149; to inhibit neurons expressing hM4Di) 30 minutes prior to a social interaction test. Three days later, mice that previously were treated with saline received an I.P. injection of CNO, and mice that were previously treated with CNO received an I.P. injection of saline, 30 minutes prior to another social interaction. Rates of USV production and non-vocal social behaviors were compared between saline and CNO days within animals to assess the effects of neuronal inhibition on social behaviors. Control mice received unilateral injections into the POA of a Cre-dependent AAV driving the expression of GFP (AAV2/1-CAG-FLEX-EGFP) and were otherwise treated identically to experimental animals.

Neuronal ablation

To permanently ablate neurons, TRAP2;Ai14 female mice received bilateral injections of an AAV2/5-ef1alpha-FLEX-taCasp3-TEVp virus into the POA. Following a three-week recovery period, these animals were individually housed for three days and subsequently given a 30-minute social encounter with a novel, group-housed female visitor. Subject mice then received an I.P. injection of 4-OHT to enable expression of caspase in activity-defined POA neurons. Two weeks later, females were single-housed for three days and then given a second 30-minute social interaction test. Social behaviors of subject females were compared between the pre-ablation and post-ablation interaction tests to assess the effects of neuronal ablation.

Optogenetic activation

Female TRAP2 mice received unilateral injections into the POA of AAV-ef1α-FLEX-ChR2 (experimental) or AAV-CAG-FLEX-GFP (control). In the same surgery, an optogenetic

ferrule was implanted approximately 250 µm above the viral injection site. Three weeks later, females were single-housed for 3 days and then given a 30-minute social interaction with a novel group-housed, female visitor. Subject females then received an I.P. injection of 4-OHT. Two weeks later, females were first placed alone in the testing chamber for a 5-minute habituation period after connecting the laser patch cable to the female's optogenetic ferrule. Optogenetic activation sessions consisted of a 5-minute period in which optogenetic activation was performed in solo females, followed by a 20-minute period in which activation was performed as subject females interacted with a novel, group-housed female visitor. The social session was further divided into three phases: 5 minutes without optogenetic activation, 10 minutes with optogenetic activation, and 5 minutes without optogenetic activation. During the middle 10 minutes of the social session, some laser stimuli were delivered at times when the two females were near to one another (inter-animal distance < ~2 mouse body lengths), and other stimuli were delivered at times when the females were not in close contact. POA_{iso} neurons were optogenetically activated with illumination from a 473 nM laser (10 mW) at 20-50 Hz (10-20 ms pulses, trains lasted 5-10s) Laser stimuli were driven by computer-controlled voltage pulses (Spike 2 version 10.8, CED).

Anatomical tracing

Female TRAP2 mice used as GFP controls in the chemogenetic inhibition experiments were subsequently used for anterograde mapping of the axonal projections of POA_{iso} neurons. Three weeks following unilateral injection into the POA of a Cre-dependent AAV driving the expression of GFP (AAV2/1-CAG-FLEX-EGFP), females were single-housed for 3 days and subsequently given a 30-minute social interaction test. Subject mice then received an I.P. injection of 4-OHT. Six weeks later, females were perfused, brains were collected and sectioned, and a confocal microscope was used to image GFP-positive axon terminals within coronal brain tissue sections.

To examine the overlap between PAG-projecting POA neurons and Fos expression, Ai14 females first received a unilateral injection into the PAG of an AAV driving the retrograde expression of Cre-recombinase (AAVrg-pgk-Cre). Two weeks later, these females were given a 30-minute social interaction test. Ninety minutes after the test, subject females were perfused, brains were collected, and coronal brain sections containing the POA were collected for Fos immunohistochemistry as described above. Brain tissue sections were imaged with a 10x objective on a Zeiss 900 laser scanning confocal microscope, and POA neurons that were Fos-positive and tdTomato-positive were counted manually by trained observers.

Statistics

Two-sided statistical comparisons were used in all analyses (alpha = 0.05). The Shapiro-Wilk test was performed to analyze the normality of each data distribution, and non-parametric statistical tests were used for comparisons that included non-normally distributed data. No statistical methods were used to pre-determine sample size. Mice were only excluded from analysis in cases in which viral injections were not targeted accurately. Details of the statistical analyses used in this study are included in Table S1.

Supplemental Information

Figure S1. Additional characterization of Fos expression in single-housed vs. group-housed females and comparison to rates of female social behaviors. (A) Representative confocal images show Fos expression (green) in the VMH of a group-housed female (left) and a single-housed female (right) following same-sex social interactions. Blue, Neurotrace. (B) Same as (A), for the caudolateral PAG. (C) Left, the relationship between total time spent in resident-initiated social investigation and numbers of Fos-positive POA neurons is shown for group-housed (teal) and single-housed (maroon) female residents following interactions with novel females. Middle, same as left, for total resident-initiated mounting time vs. numbers of Fos-positive POA neurons. Data only shown for single-housed residents because group-housed residents never mounted female visitors. Right, same as left, for total USVs vs. numbers of Fos-positive POA neurons. (D) Left, the relationship between total time spent in resident-initiated social investigation and numbers of Fos-positive VMH neurons is shown for group-housed (teal) and single-housed (maroon) female residents following interactions with novel females. Middle, same as left, for total resident-initiated mounting time vs. numbers of Fos-positive VMH neurons. Right, same as left, for total USVs vs. numbers of Fos-positive VMH neurons. (E) Left, the relationship between total time spent in resident-initiated social investigation and numbers of Fos-positive caudolateral PAG neurons is shown for group-housed (teal) and single-housed (maroon) female residents following interactions with novel females. Middle, same as left, for total resident-initiated mounting time vs. numbers of Fos-positive PAG neurons. Right, same as left, for total USVs vs. numbers of Fos-positive PAG neurons.

Figure S2. Characterization of neurotransmitter phenotype and axonal projections of POA_{iso} neurons. (A) Representative confocal images of in situ hybridization performed on brain sections containing the POA, showing overlap of expression of Fos (green) and VGAT (magenta). Blue, DAPI. (B) Quantification of proportion of Fos-positive POA neurons that expressed VGAT. (C) Experimental timeline and viral strategy to express GFP in POA_{iso} neurons. (D) Confocal images showing GFP-labeled axons of POA_{iso} neurons within the caudolateral PAG. Blue, Neurotrace. (E) Experimental timeline and viral strategy to retrogradely label PAG-projecting POA neurons with tdTomato. (F) Confocal image showing tdTomato labeling in a coronal section containing the POA, and dotted circles in insets indicate examples of double-labeled neurons. Neurotrace, blue. (G) Quantification of proportion of tdTomato-expressing POA neurons that are also Fos-positive.

Table S1. Details of statistical analyses.

References

Alger SJ, Riters LV. 2006. Lesions to the medial preoptic nucleus differentially affect singing and nest box-directed behaviors within and outside of the breeding season in European starlings (Sturnus vulgaris). *Behav Neurosci* **120**:1326–1336. doi:10.1037/0735-7044.120.6.1326

Allen WE, DeNardo LA, Chen MZ, Liu CD, Loh KM, Fenno LE, Ramakrishnan C, Deisseroth K, Luo L. 2017. Thirst-associated preoptic neurons encode an aversive motivational drive. *Science* **357**:1149–1155. doi:10.1126/science.aan6747

An D, Chen W, Yu D-Q, Wang S-W, Yu W-Z, Xu H, Wang D-M, Zhao D, Sun Y-P, Wu J-C, Tang Y-Y, Yin S-M. 2017. Effects of social isolation, re-socialization and age on cognitive and aggressive behaviors of Kunming mice and BALB/c mice. *Anim Sci J* **88**:798–806. doi:10.1111/asj.12688

Arrigo BA, Bullock JL. 2008. The psychological effects of solitary confinement on prisoners in supermax units: reviewing what we know and recommending what should change. *Int J Offender Ther Comp Criminol* **52**:622–640. doi:10.1177/0306624X07309720

Bariselli S, Hörnberg H, Prévost-Solié C, Musardo S, Hatstatt-Burklé L, Scheiffele P, Bellone C. 2018. Role of VTA dopamine neurons and neuroligin 3 in sociability traits related to nonfamiliar conspecific interaction. *Nat Commun* **9**:3173. doi:10.1038/s41467-018-05382-3

Baumeister RF, Leary MR. 1995. The need to belong: Desire for interpersonal attachments as a fundamental human motivation. *Psychol Bull* **117**:497–529. doi:10.1037/0033-2909.117.3.497

Bean NY, Nunez AA, Conner R. 1981. Effects of medial preoptic lesions on male mouse ultrasonic vocalizations and copulatory behavior. *Brain Res Bull* **6**:109–112. doi:10.1016/s0361-9230(81)80033-0

Cacioppo JT, Cacioppo S. 2018. Chapter Three - Loneliness in the Modern Age: An Evolutionary Theory of Loneliness (ETL) In: Olson JM, editor. Advances in Experimental Social Psychology. Academic Press. pp. 127–197. doi:10.1016/bs.aesp.2018.03.003

Cacioppo JT, Hughes ME, Waite LJ, Hawkley LC, Thisted RA. 2006. Loneliness as a specific risk factor for depressive symptoms: cross-sectional and longitudinal analyses. *Psychol Aging* **21**:140–151. doi:10.1037/0882-7974.21.1.140

Check JVP, Perlman D, Malamuth NM. 1985. Loneuness and Aggressive Behaviour. *J Sol Pers Relat* **2**:243–252. doi:10.1177/0265407585023001

Chen J, Markowitz JE, Lilascharoen V, Taylor S, Sheurpukdi P, Keller JA, Jensen JR, Lim BK, Datta SR, Stowers L. 2021. Flexible scaling and persistence of social vocal communication. *Nature* **593**:108–113. doi:10.1038/s41586-021-03403-8

Chevallier C, Kohls G, Troiani V, Brodkin ES, Schultz RT. 2012. The Social Motivation Theory of Autism. *Trends Cogn Sci* **16**:231–239. doi:10.1016/j.tics.2012.02.007

Clements CC, Zoltowski AR, Yankowitz LD, Yerys BE, Schultz RT, Herrington JD. 2018. Evaluation of the Social Motivation Hypothesis of Autism. *JAMA Psychiatry* **75**:797–808. doi:10.1001/jamapsychiatry.2018.1100

Dai B, Sun F, Tong X, Ding Y, Kuang A, Osakada T, Li Y, Lin D. 2022. Responses and functions of dopamine in nucleus accumbens core during social behaviors. *Cell Rep* **40**:111246. doi:10.1016/j.celrep.2022.111246

DeNardo LA, Liu CD, Allen WE, Adams EL, Friedmann D, Fu L, Guenthner CJ, Tessier-Lavigne M, Luo L. 2019. Temporal Evolution of Cortical Ensembles Promoting Remote Memory Retrieval. *Nat Neurosci* **22**:460–469. doi:10.1038/s41593-018-0318-7

Dölen G, Darvishzadeh A, Huang KW, Malenka RC. 2013. Social reward requires coordinated activity of nucleus accumbens oxytocin and serotonin. *Nature* **501**:179–184. doi:10.1038/nature12518

Floody OR. 1989. Dissociation of hypothalamic effects on ultrasound production and copulation. *Physiol Behav* **46**:299–307. doi:10.1016/0031-9384(89)90271-0

Fukumitsu K, Huang AJ, McHugh TJ, Kuroda KO. 2023. Role of Calcr expressing neurons in the medial amygdala in social contact among females. *Mol Brain* **16**:10. doi:10.1186/s13041-023-00993-4

Fukumitsu K, Kaneko M, Maruyama T, Yoshihara C, Huang AJ, McHugh TJ, Itohara S, Tanaka M, Kuroda KO. 2022. Amylin-Calcitonin receptor signaling in the medial preoptic area mediates affiliative social behaviors in female mice. *Nat Commun* **13**:709. doi:10.1038/s41467-022-28131-z

Gao S-C, Wei Y-C, Wang S-R, Xu X-H. 2019. Medial Preoptic Area Modulates Courtship Ultrasonic Vocalization in Adult Male Mice. *Neurosci Bull* **35**:697–708. doi:10.1007/s12264-019-00365-w

Green DB, Shackleton TM, Grimsley JMS, Zobay O, Palmer AR, Wallace MN. 2018. Communication calls produced by electrical stimulation of four structures in the guinea pig brain. *PLoS One* **13**:e0194091. doi:10.1371/journal.pone.0194091

Gunaydin LA, Grosenick L, Finkelstein JC, Kauvar IV, Fenno LE, Adhikari A, Lammel S, Mirzabekov JJ, Airan RD, Zalocusky KA, Tye KM, Anikeeva P, Malenka RC, Deisseroth K. 2014. Natural neural projection dynamics underlying social behavior. *Cell* **157**:1535–1551. doi:10.1016/j.cell.2014.05.017

Hashikawa K, Hashikawa Y, Tremblay R, Zhang J, Feng JE, Sabol A, Piper WT, Lee H, Rudy B, Lin D. 2017. Esr1+ cells in the ventromedial hypothalamus control female aggression. *Nat Neurosci* **20**:1580-1590. doi:10.1038/nn.4644

Hossain MM, Sultana A, Purohit N. 2020. Mental health outcomes of quarantine and isolation for infection prevention: a systematic umbrella review of the global evidence. *Epidemiol Health* **42**. doi:10.4178/epih.e2020038

House JS, Landis KR, Umberson D. 1988. Social relationships and health. *Science* **241**:540–545. doi:10.1126/science.3399889

Hu RK, Zuo Y, Ly T, Wang J, Meera P, Wu YE, Hong W. 2021. An amygdala-to-hypothalamus circuit for social reward. *Nat Neurosci* **24**:831–842. doi:10.1038/s41593-021-00828-2

Hung LW, Neuner S, Polepalli JS, Beier KT, Wright M, Walsh JJ, Lewis EM, Luo L, Deisseroth K, Dölen G, Malenka RC. 2017. Gating of social reward by oxytocin in the ventral tegmental area. *Science* **357**:1406–1411. doi:10.1126/science.aan4994

Inagaki TK, Muscatell KA, Moieni M, Dutcher JM, Jevtic I, Irwin MR, Eisenberger NI. 2016. Yearning for connection? Loneliness is associated with increased ventral striatum activity to close others. *Soc Cogn Affect Neurosci* **11**:1096–1101. doi:10.1093/scan/nsv076

Jürgens U. 1994. The role of the periaqueductal grey in vocal behaviour. *Behav Brain Res* **62**:107–117. doi:10.1016/0166-4328(94)90017-5

Karigo T, Kennedy A, Yang B, Liu M, Tai D, Wahle IA, Anderson DJ. 2021. Distinct hypothalamic control of same- and opposite-sex mounting behaviour in mice. *Nature* **589**:258–263. doi:10.1038/s41586-020-2995-0

Killgore WDS, Cloonan SA, Taylor EC, Anlap I, Dailey NS. 2021. Increasing aggression during the COVID-19 lockdowns. *J Affect Disord Rep* **5**:100163. doi:10.1016/j.jadr.2021.100163

Kohl J, Babayan BM, Rubinstein ND, Autry AE, Marin-Rodriguez B, Kapoor V, Miyamishi K, Zweifel LS, Luo L, Uchida N, Dulac C. 2018. Functional circuit architecture underlying parental behaviour. *Nature* **556**:326–331. doi:10.1038/s41586-018-0027-0

Lee CR, Chen A, Tye KM. 2021. The neural circuitry of social homeostasis: Consequences of acute versus chronic social isolation. *Cell* **184**:1500–1516. doi:10.1016/j.cell.2021.02.028

Lee H, Kim D-W, Remedios R, Anthony TE, Chang A, Madisen L, Zeng H, Anderson DJ. 2014. Scalable control of mounting and attack by Esr1+ neurons in the ventromedial hypothalamus. *Nature* **509**:627–632. doi:10.1038/nature13169

Liu D, Rahman M, Johnson A, Tsutsui-Kimura I, Pena N, Talay M, Logeman BL, Finkbeiner S, Choi S, Capo-Battaglia A, Abdus-Saboor I, Ginty DD, Uchida N, Watabe-Uchida M, Dulac C. 2023. A Hypothalamic Circuit Underlying the Dynamic Control of Social Homeostasis. Preprint at bioRxiv. doi:10.1101/2023.05.19.540391

Liu M, Kim D-W, Zeng H, Anderson DJ. 2022. Make war not love: The neural substrate underlying a state-dependent switch in female social behavior. *Neuron* **110**:841-856.e6. doi:10.1016/j.neuron.2021.12.002

Love TM. 2014. Oxytocin, motivation and the role of dopamine. *Pharmacol Biochem Behav* **119**:49–60. doi:10.1016/j.pbb.2013.06.011

Ma X, Jiang D, Jiang W, Wang F, Jia M, Wu J, Hashimoto K, Dang Y, Gao C. 2011. Social isolation-induced aggression potentiates anxiety and depressive-like behavior in male mice subjected to unpredictable chronic mild stress. *PLoS One* **6**:e20955. doi:10.1371/journal.pone.0020955

Ma Y-K, Zeng P-Y, Chu Y-H, Lee C-L, Cheng C-C, Chen C-H, Su Y-S, Lin K-T, Kuo T-H. 2022. Lack of social touch alters anxiety-like and social behaviors in male mice. *Stress* **25**:134–144. doi:10.1080/10253890.2022.2047174

Machimbarrena JM, Álvarez-Bardón A, León-Mejía A, Gutiérrez-Ortega M, Casadiego-Cabrales A, González-Cabrera J. 2019. Loneliness and Personality Profiles Involved in Bullying Victimization and Aggressive Behavior. *School Ment Health* **11**:807–818. doi:10.1007/s12310-019-09328-y

Matsumoto K, Pinna G, Puia G, Guidotti A, Costa E. 2005. Social isolation stress-induced aggression in mice: a model to study the pharmacology of neurosteroidogenesis. *Stress* **8**:85–93. doi:10.1080/10253890500159022

Matthews GA, Nieh EH, Vander Weele CM, Halbert SA, Pradhan RV, Yosafat AS, Glober GF, Izadmehr EM, Thomas RE, Lacy GD, Wildes CP, Ungless MA, Tye KM. 2016. Dorsal Raphe Dopamine Neurons Represent the Experience of Social Isolation. *Cell* **164**:617–631. doi:10.1016/j.cell.2015.12.040

McHenry JA, Otis JM, Rossi MA, Robinson JE, Kosyk O, Miller NW, McElligott ZA, Budygin EA, Rubinow DR, Stuber GD. 2017. Hormonal gain control of a medial preoptic area social reward circuit. *Nat Neurosci* **20**:449–458. doi:10.1038/nn.4487

McWain MA, Pace RL, Nalan PA, Lester DB. 2022. Age-dependent effects of social isolation on mesolimbic dopamine release. *Exp Brain Res* **240**:2803–2815. doi:10.1007/s00221-022-06449-w

Mears DP, Bales WD. 2009. Supermax Incarceration and Recidivism. *Criminology* **47**:1131–1166. doi:10.1111/j.1745-9125.2009.00171.x

Melis MR, Sanna F, Argiolas A. 2022. Dopamine, Erectile Function and Male Sexual Behavior from the Past to the Present: A Review. *Brain Sci* **12**:826. doi:10.3390/brainsci12070826

Merari A, Ginton A. 1975. Characteristics of exaggerated sexual behavior induced by electrical stimulation of the medial preoptic area in male rats. *Brain Res* **86**:97–108. doi:10.1016/0006-8993(75)90641-1

Michael V, Goffinet J, Pearson J, Wang F, Tschida K, Mooney R. 2020. Circuit and synaptic organization of forebrain-to-midbrain pathways that promote and suppress vocalization. *Elife* **9**:e63493. doi:10.7554/eLife.63493

Musardo S, Contestabile A, Knoop M, Baud O, Bellone C. 2022. Oxytocin neurons mediate the effect of social isolation via the VTA circuits. *eLife* **11**:e73421. doi:10.7554/eLife.73421

Niesink RJ, van Ree JM. 1982. Short-term isolation increases social interactions of male rats: a parametric analysis. *Physiol Behav* **29**:819–825. doi:10.1016/0031-9384(82)90331-6

Otchy TM, Wolff SBE, Rhee JY, Pehlevan C, Kawai R, Kempf A, Gobes SMH, Ölveczky BP. 2015. Acute off-target effects of neural circuit manipulations. *Nature* **528**:358–363. doi:10.1038/nature16442

Panksepp J, Beatty WW. 1980. Social deprivation and play in rats. *Behav Neural Biol* **30**:197–206. doi:10.1016/s0163-1047(80)91077-8

Reid JA, Chenneville T, Gardy SM, Baglivio MT. 2022. An Exploratory Study of COVID-19's Impact on Psychological Distress and Antisocial Behavior Among Justice-Involved Youth. *Crime Delinquency* **68**:1271–1291. doi:10.1177/00111287211054729

Resendez SL, Namboodiri VMK, Otis JM, Eckman LEH, Rodriguez-Romaguera J, Ung RL, Basiri ML, Kosyk O, Rossi MA, Dichter GS, Stuber GD. 2020. Social Stimuli Induce Activation of Oxytocin Neurons Within the Paraventricular Nucleus of the Hypothalamus to Promote Social Behavior in Male Mice. *J Neurosci* **40**:2282–2295. doi:10.1523/JNEUROSCI.1515-18.2020

Riters LV. 2012. The role of motivation and reward neural systems in vocal communication in songbirds. *Front Neuroendocrinol* **33**:194–209. doi:10.1016/j.yfrne.2012.04.002

Riters LV, Ball GF. 1999. Lesions to the medial preoptic area affect singing in the male European starling (Sturnus vulgaris). *Horm Behav* **36**:276–286. doi:10.1006/hbeh.1999.1549

Riters LV, Eens M, Pinxten R, Duffy DL, Balthazart J, Ball GF. 2000. Seasonal changes in courtship song and the medial preoptic area in male European starlings (Sturnus vulgaris). *Horm Behav* **38**:250–261. doi:10.1006/hbeh.2000.1623

Robinson DL, Zitzman DL, Smith KJ, Spear LP. 2011. Fast dopamine release events in the nucleus accumbens of early adolescent rats. *Neuroscience* **176**:296–307. doi:10.1016/j.neuroscience.2010.12.016

Solié C, Girard B, Righetti B, Tapparel M, Bellone C. 2022. VTA dopamine neuron activity encodes social interaction and promotes reinforcement learning through social prediction error. *Nat Neurosci* **25**:86–97. doi:10.1038/s41593-021-00972-9

Tan T, Wang W, Liu T, Zhong P, Conrow-Graham M, Tian X, Yan Z. 2021. Neural circuits and activity dynamics underlying sex-specific effects of chronic social isolation stress. *Cell Rep* **34**:108874. doi:10.1016/j.celrep.2021.108874

Tang Y, Chen Z, Tao H, Li C, Zhang X, Tang A, Liu Y. 2014. Oxytocin activation of neurons in ventral tegmental area and interfascicular nucleus of mouse midbrain. *Neuropharmacology* **77**:277–284. doi:10.1016/j.neuropharm.2013.10.004

Tomova L, Wang KL, Thompson T, Matthews GA, Takahashi A, Tye KM, Saxe R. 2020. Acute social isolation evokes midbrain craving responses similar to hunger. *Nat Neurosci* **23**:1597–1605. doi:10.1038/s41593-020-00742-z

Toth M, Mikics E, Tulogdi A, Aliczki M, Haller J. 2011. Post-weaning social isolation induces abnormal forms of aggression in conjunction with increased glucocorticoid and autonomic stress responses. *Horm Behav* **60**:28–36. doi:10.1016/j.yhbeh.2011.02.003

Tschida K, Michael V, Takatoh J, Han B-X, Zhao S, Sakurai K, Mooney R, Wang F. 2019. A Specialized Neural Circuit Gates Social Vocalizations in the Mouse. *Neuron* **103**:459-472.e4. doi:10.1016/j.neuron.2019.05.025

Valzelli L. 1973. The “isolation syndrome” in mice. *Psychopharmacologia* **31**:305–320. doi:10.1007/BF00421275

Walum H, Young LJ. 2018. The neural mechanisms and circuitry of the pair bond. *Nat Rev Neurosci* **19**:643–654. doi:10.1038/s41583-018-0072-6

Warren MR, Clein RS, Spurrier MS, Roth ED, Neunuebel JP. 2020. Ultrashort-range, high-frequency communication by female mice shapes social interactions. *Sci Rep* **10**:2637. doi:10.1038/s41598-020-59418-0

Wei Y-C, Wang S-R, Jiao Z-L, Zhang W, Lin J-K, Li X-Y, Li S-S, Zhang X, Xu X-H. 2018. Medial preoptic area in mice is capable of mediating sexually dimorphic behaviors regardless of gender. *Nat Commun* **9**:279. doi:10.1038/s41467-017-02648-0

Weiss IC, Pryce CR, Jongen-Rêlo AL, Nanz-Bahr NI, Feldon J. 2004. Effect of social isolation on stress-related behavioural and neuroendocrine state in the rat. *Behav Brain Res* **152**:279–295. doi:10.1016/j.bbr.2003.10.015

Wiberg GS, Grice HC. 1963. Long-term isolation stress in rats. *Science* **142**:507. doi:10.1126/science.142.3591.507

Wu YE, Dang J, Kingsbury L, Zhang M, Sun F, Hu RK, Hong W. 2021. Neural control of affiliative touch in prosocial interaction. *Nature* **599**:262–267. doi:10.1038/s41586-021-03962-w

Xiao L, Priest MF, Nasenbeny J, Lu T, Kozorovitskiy Y. 2017. Biased Oxytocinergic Modulation of Midbrain Dopamine Systems. *Neuron* **95**:368-384.e5. doi:10.1016/j.neuron.2017.06.003

Yorgason JT, Calipari ES, Ferris MJ, Karkhanis AN, Fordahl SC, Weiner JL, Jones SR. 2016. Social isolation rearing increases dopamine uptake and psychostimulant potency in the striatum. *Neuropharmacology* **101**:471–479. doi:10.1016/j.neuropharm.2015.10.025

Zelikowsky M, Hui M, Karigo T, Choe A, Yang B, Blanco MR, Beadle K, Gradinaru V, Deverman BE, Anderson DJ. 2018. The Neuropeptide Tac2 Controls a Distributed Brain State Induced by Chronic Social Isolation Stress. *Cell* **173**:1265-1279.e19. doi:10.1016/j.cell.2018.03.037

Zhao X, Ziobro P, Pranic NM, Chu S, Rabinovich S, Chan W, Zhao J, Kornbrek C, He Z, Tschida KA. 2021. Sex- and context-dependent effects of acute isolation on vocal and non-vocal social behaviors in mice. *PLoS One* **16**:e0255640. doi:10.1371/journal.pone.0255640

Figure 1.

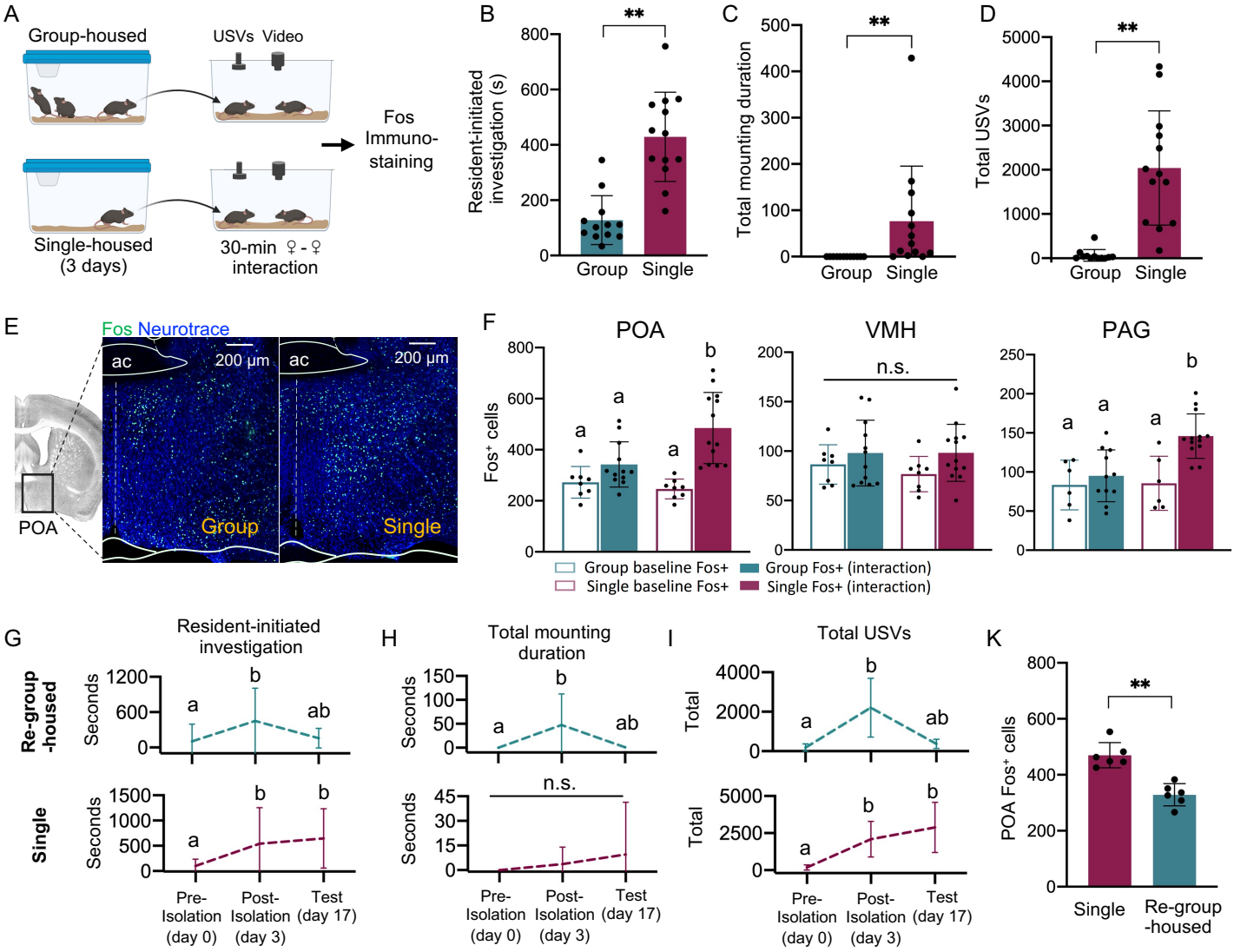
A
Group-housed
USVs Video
Fos Immuno-staining
Single-housed (3 days)
30-min ♀-♀ interaction
B
Resident-initiated investigation (s)
Group
Single
C
Total mounting duration
D
Total USVs
E
Fos Neurotrace
ac
200 µm
POA
Group
Single
F
POA
VMH
PAG
Fos+ cells
n.s.
Group baseline Fos+
Single baseline Fos+
Group Fos+ (interaction)
Single Fos+ (interaction)
G
Resident-initiated investigation
Re-group -housed
Single
Seconds
Pre-Isolation (day 0)
Post-Isolation (day 3)
Test (day 17)
H
Total mounting duration
I
Total USVs
Total
K
POA Fos+ cells
Single
Re-group -housed

Figure 2.

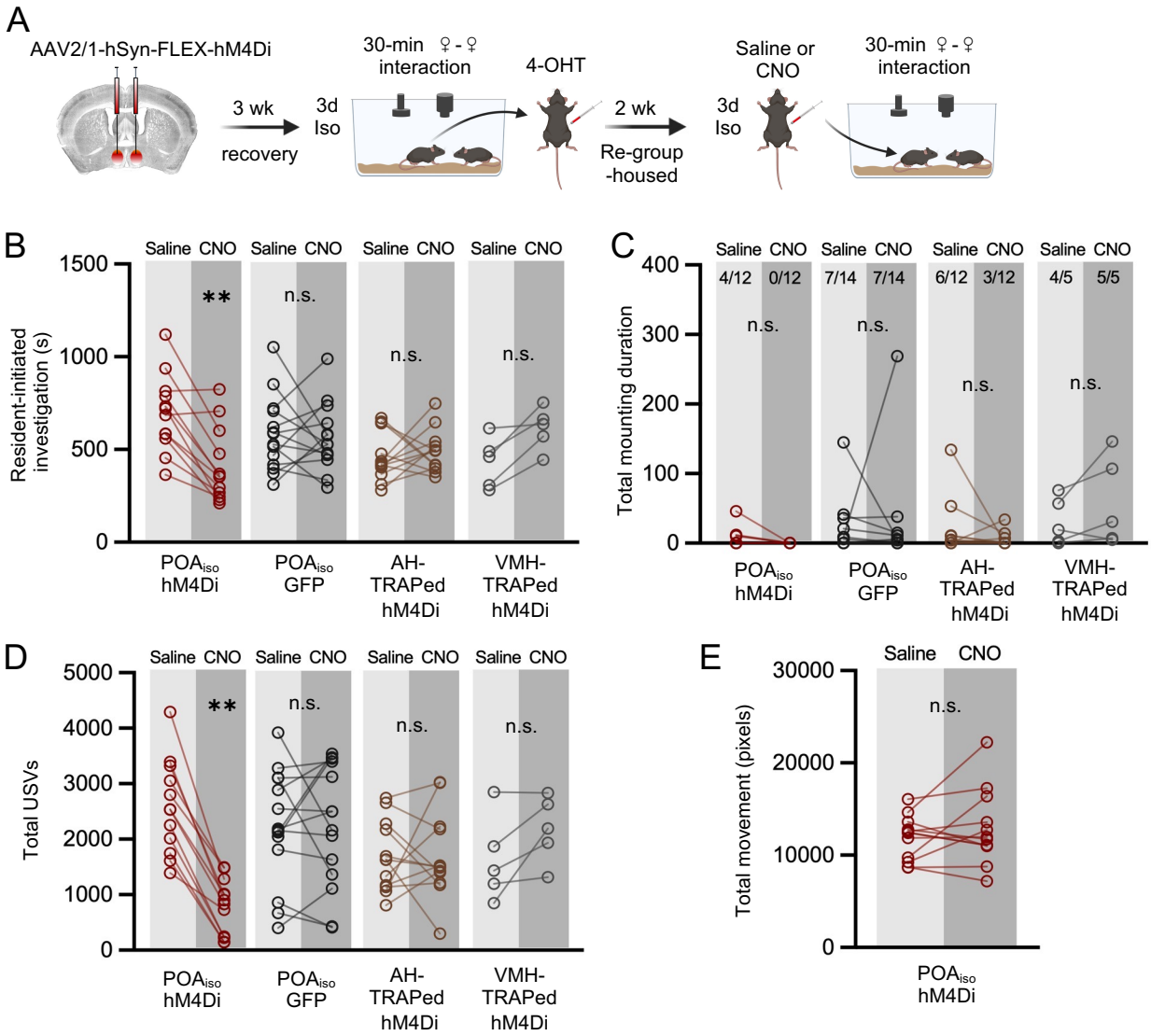
A
AAV2/1-hSyn-FLEX-hM4Di
3 wk
recovery
3d
Iso
30-min ♀-♀
interaction
4-OHT
2 wk
Re-group
-housed
3d
Iso
Saline or
CNO
30-min ♀-♀
interaction
B
Saline CNO
Resident-initiated investigation (s)
1500
1000
500
0
**
n.s.
POAiso hM4Di
POAiso GFP
AH-TRAPed hM4Di
VMH-TRAPed hM4Di
C
Total mounting duration
400
300
200
100
0
4/12
0/12
7/14
7/14
6/12
3/12
4/5
5/5
D
Total USVs
5000
4000
3000
2000
1000
0
E
Total movement (pixels)
30000
20000
10000
0
Saline
CNO

Figure 3.

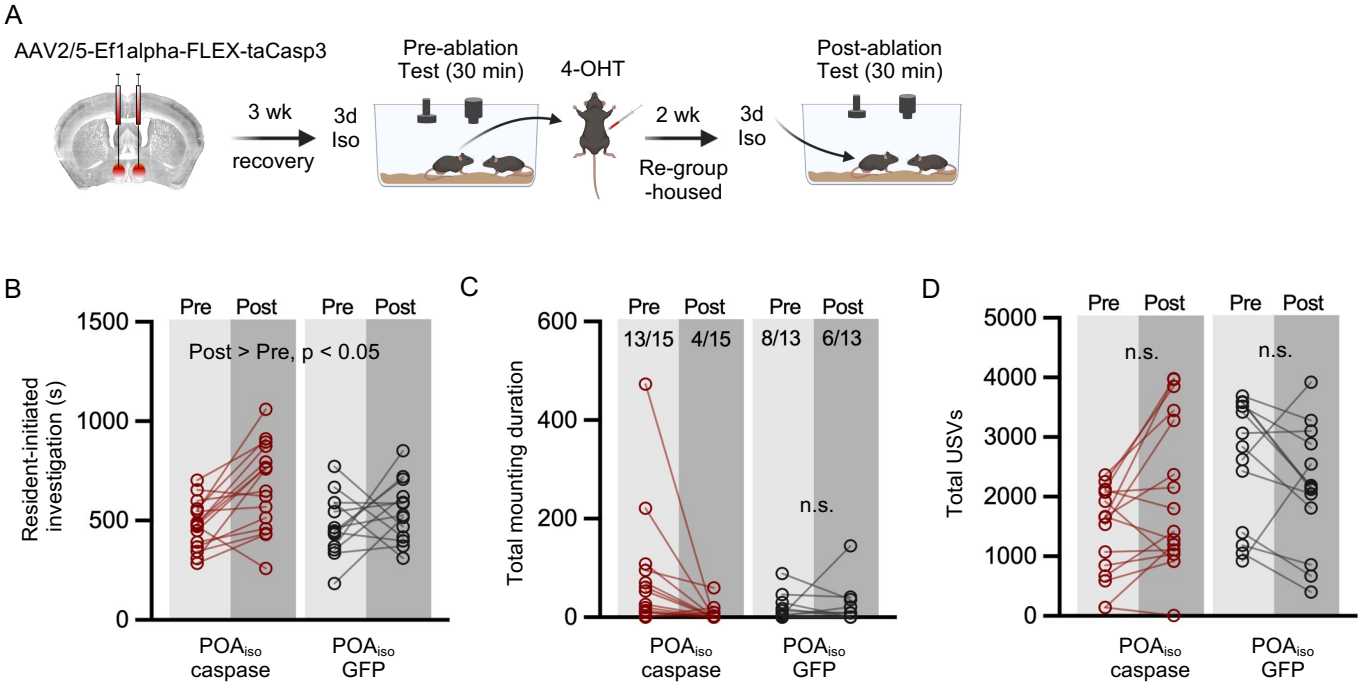
A
AAV2/5-Ef1alpha-FLEX-taCasp3
3 wk
recovery
3d
Iso
Pre-ablation
Test (30 min)
4-OHT
2 wk
Re-group
-housed
3d
Iso
Post-ablation
Test (30 min)
B
Resident-initiated investigation (s)
1500
1000
500
0
Pre
Post
Pre
Post
Post > Pre, p < 0.05
POAiso caspase
POAiso GFP
C
Total mounting duration
600
400
200
0
Pre
Post
Pre
Post
13/15
4/15
8/13
6/13
n.s.
POAiso caspase
POAiso GFP
D
Total USVs
5000
4000
3000
2000
1000
0
Pre
Post
Pre
Post
n.s.
n.s.
POAiso caspase
POAiso GFP

Figure 4

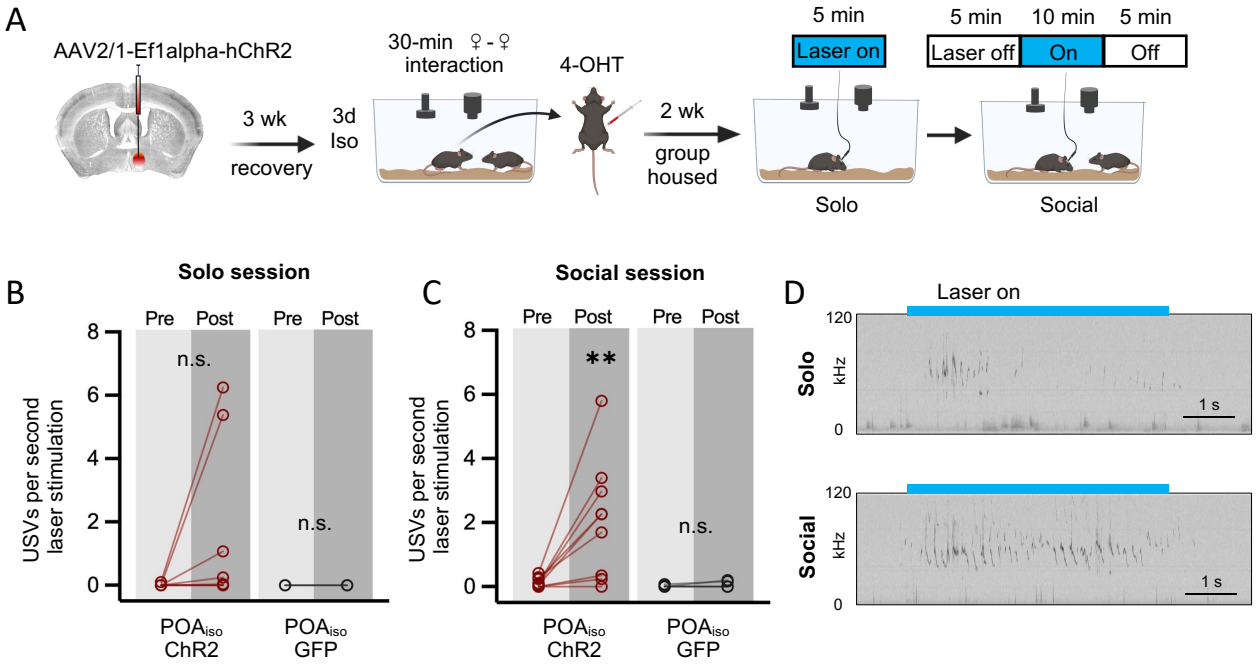
A
AAV2/1-Ef1alpha-hChR2
3 wk
recovery
3d
Iso
30-min ♀-♀
interaction
4-OHT
2 wk
group
housed
5 min
Laser on
Solo
5 min
Laser off
10 min
On
5 min
Off
Social
B
Solo session
Pre
Post
Pre
Post
n.s.
n.s.
USVs per second
laser stimulation
POAiso
ChR2
POAiso
GFP
C
Social session
Pre
Post
Pre
Post
**
n.s.
USVs per second
laser stimulation
POAiso
ChR2
POAiso
GFP
D
Laser on
Solo
Social
120
kHz
0
1 s

Figure 5.

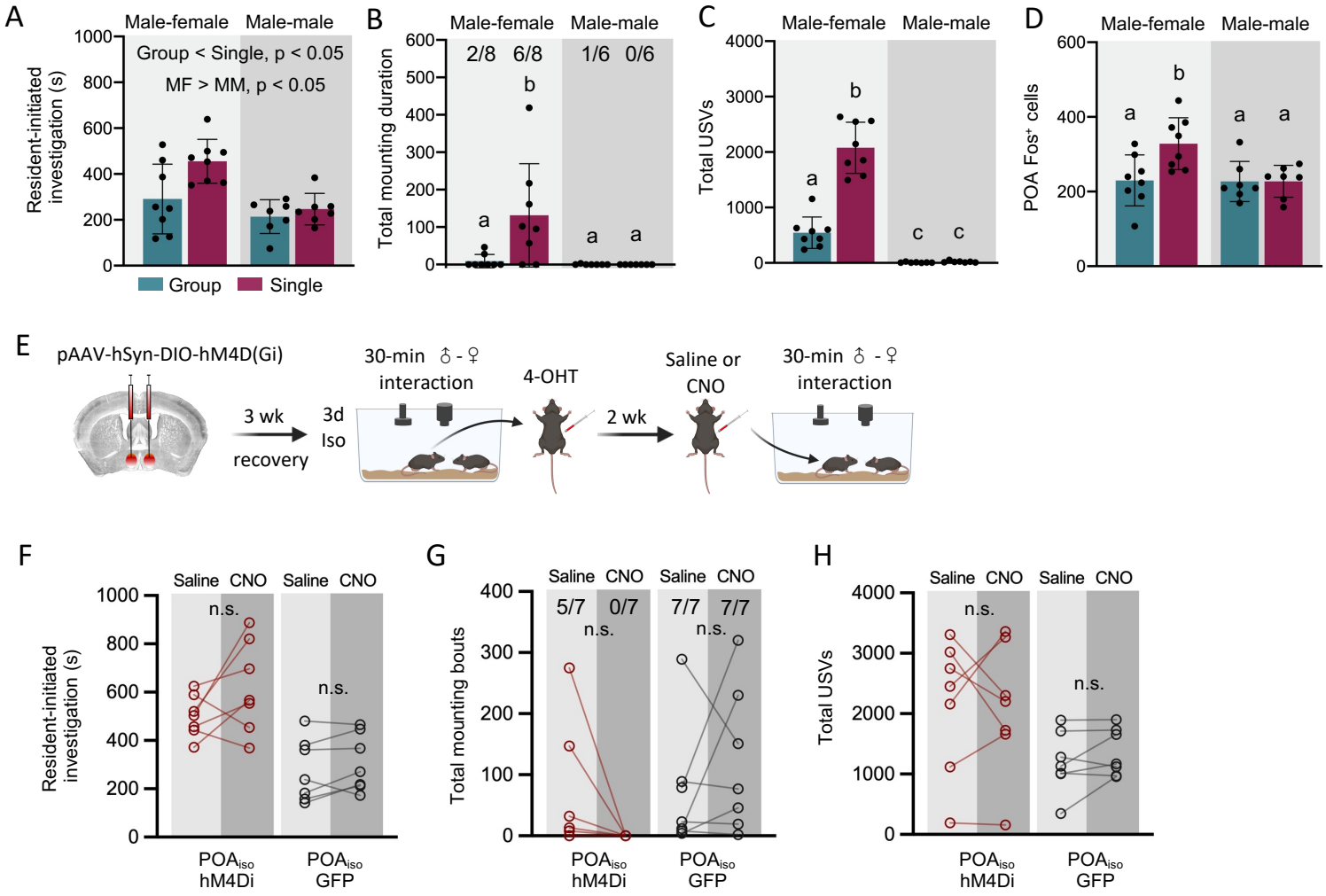
A
Male-female
Male-male
Group < Single, p < 0.05
MF > MM, p < 0.05
Resident-initiated investigation (s)
Group
Single
B
Male-female
Male-male
2/8
6/8
1/6
0/6
Total mounting duration
C
Male-female
Male-male
Total USVs
D
Male-female
Male-male
POA Fos⁺ cells
E
pAAV-hSyn-DIO-hM4D(Gi)
3 wk
recovery
3d
Iso
30-min ♂-♀
interaction
4-OHT
2 wk
Saline or
CNO
30-min ♂-♀
interaction
F
Saline
CNO
n.s.
Resident-initiated investigation (s)
POAiso hM4Di
POAiso GFP
G
5/7
0/7
7/7
7/7
Total mounting bouts
H
Total USVs